

# Toward Complete Resolution of DNA/Carbon Nanotube Hybrids by Aqueous Two-Phase Systems

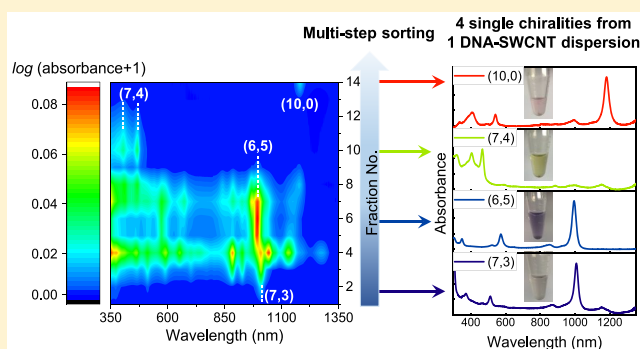
Min Lyu,<sup>†</sup> Brendan Meany,<sup>‡</sup> Juan Yang,<sup>\*,†</sup> Yan Li,<sup>\*,†</sup> and Ming Zheng<sup>\*,‡</sup>

<sup>†</sup>Beijing National Laboratory for Molecular Science, Key Laboratory for the Physics and Chemistry of Nanodevices, State Key Laboratory of Rare Earth Materials Chemistry and Applications, College of Chemistry and Molecular Engineering, Peking University, Beijing 100871, China

<sup>‡</sup>Materials Science and Engineering Division, National Institute of Standards and Technology, 100 Bureau Drive, Gaithersburg, Maryland 20899, United States

## Supporting Information

**ABSTRACT:** Sequence-dependent interactions between DNA and single-wall carbon nanotubes (SWCNTs) are shown to provide resolution for the atomic-structure-based sorting of DNA-wrapped SWCNTs. Previous studies have demonstrated that aqueous two-phase (ATP) systems are very effective for sorting DNA-wrapped SWCNTs (DNA-SWCNTs). However, most separations have been carried out with a polyethylene glycol (PEG)/polyacrylamide (PAM) ATP system, which shows severe interfacial trapping for many DNA-SWCNT dispersions, resulting in significant material loss and limiting multistage extraction. Here, we report a study of several new ATP systems for sorting DNA-SWCNTs. We have developed a convenient method to explore these systems without knowledge of the corresponding phase diagram. We further show that the molecular weight of the polymer strongly affects the partition behavior and separation results for DNA-SWCNTs in PEG/dextran (DX) ATP systems. This leads to the identification of the PEG1.5kDa/DX250kDa ATP system as an effective vehicle for the chirality separation of DNA-SWCNTs. Additionally, this ATP system exhibits greatly reduced interfacial trapping, enabling for the first time continuous multistep sorting of four species of SWCNTs from a single dispersion. Enhanced stability of DNA-SWCNTs in the PEG1.5kDa/DX250kDa ATP system also allows us to investigate pH dependent sorting of SWCNTs wrapped by C-rich sequences. Our observations suggest that hydrogen bonding may form between the DNA bases at lower pH, enabling a more ordered wrapping structure on the SWCNTs and improvement in sorting (11,0). Together, these findings reveal that the new ATP system is suitable for searching DNA sequences leading toward more complete resolution of DNA-SWCNTs. A new concept of “resolving sequences”, evolved from the old notion of “recognition sequences”, is proposed to describe a broader range of behaviors of DNA/SWCNT interactions and sorting.



## INTRODUCTION

Single-wall carbon nanotubes (SWCNTs) are a family of molecules of cylindrical shape with different chiralities.<sup>1</sup> Single-stranded DNA (ssDNA)<sup>2–7</sup> has been found to be effective for the dispersion of SWCNTs through  $\pi$ – $\pi$  stacking between the DNA base and the surface of SWCNTs. The DNA wrapped on SWCNTs enables programmable assembly of DNA-SWCNTs hybrids, which represents a new approach that could pave the way toward complex devices and circuits.<sup>8–12</sup> The specific shape and size of the exposed surface of SWCNTs determined by the structure-defined DNA wrapping enable their application in molecular sensing.<sup>13–18</sup> Real-time detection<sup>19</sup> and in vivo optical quantification<sup>20</sup> based on DNA-SWCNT hybrids show advantages in terms of the single-molecule sensitivity<sup>16,17,19</sup> and multiplex detection capability.<sup>13,17,19,21</sup> As all commercially available SWCNT raw materials are mixtures of various chiralities, most studies of DNA-SWCNTs are based

on mixtures of different chiralities. Efforts on SWCNT sorting started in 2003, resulting in development of a number of methods including ion exchange chromatography (IEX),<sup>2–7</sup> density gradient ultracentrifugation,<sup>22–29</sup> selective extraction by conjugated polymers,<sup>30–33</sup> and gel chromatography.<sup>34–37</sup> In 2013, aqueous two-phase (ATP) extraction for SWCNT sorting was first reported by Khripin et al.<sup>38</sup> Since then, many publications have demonstrated that ATP extraction has unique advantages over other sorting methods of SWCNTs.<sup>39–47</sup>

The ATP extraction method, pioneered by Albertsson,<sup>48</sup> uses polymer–polymer phase separation to create two immiscible aqueous phases of slightly different physical properties. Separation based on the uneven distribution of

Received: September 14, 2019

Published: November 29, 2019

certain analytes between the top and the bottom phases can arise from their difference in solvation energy, electrostatic interaction, and biospecific affinity interaction with the two phases.<sup>49–51</sup> ATP extraction has been successfully applied in many areas such as the downstream processing of biological compounds,<sup>52–57</sup> separation of metal ions<sup>58</sup> and metal nanoparticles,<sup>59</sup> and analysis to determine the chemical properties or surface properties of the analytes.<sup>60,61</sup> Previous works on ATP separation of SWCNTs have been applied to both surfactant-dispersed SWCNTs and DNA-SWCNT dispersions. Compared with surfactants, the enormous size of the DNA library provides almost infinite ways to coat SWCNTs. It has already been shown that, once a proper DNA sequence is chosen, it will yield a top or bottom fraction with a defined handedness and helicity of the SWCNTs.<sup>44,45</sup> The sequence-dependent<sup>2–5,44,45,61–64</sup> interaction between DNA and SWCNTs enables certain special sequences to form an ordered and resolvable structure on specific SWCNT species, which is believed to be the basis of the sorting of DNA-SWCNTs. Molecular modeling<sup>3</sup> and atomic force microscopy<sup>2</sup> suggest that the DNA strands bind to the surface of SWCNTs through  $\pi$ -stacking, resulting in a helical wrapping structure. Subsequently, more sophisticated molecular dynamics (MD) simulations have also supported this picture.<sup>65–68</sup> As a new emerging technology for sorting carbon nanotubes, ATP extraction exhibits the following advantages: (1) it is easy to scale up and automated multistage separation is feasible by using counter-current chromatography;<sup>69</sup> (2) the separation process does not rely on a complicated instrument and is mainly driven by the differences in solvation energy, which exclude the need for external field; (3) it is broadly applicable to many kinds of SWCNT structures and surface functionalizations, including both surfactant-dispersed SWCNTs and DNA-SWCNTs, filled and empty SWCNTs,<sup>70,71</sup> and organic color center (OCC)-tailored SWCNTs;<sup>72</sup> and (4) it can purify SWCNTs of defined handedness and helicity covering the entire chiral angle range and all electronic types. Previous works on ATP separation of DNA-SWCNTs have been limited mainly to the PEG/PAM system. However, one serious problem is that the stability of the SWCNT dispersion in the PEG/PAM system is sensitive to the choice of DNA, and most dispersions suffer from severe interfacial trapping issues that make multistage sorting impossible. Another problem is that, unfortunately, the PAM polymer used in the original study by Ao et al.<sup>44,45</sup> has been commercially discontinued, and other commercial variations of PAM have failed to work for sorting of DNA-SWCNTs.

In this paper, we report a simple way to set up a new ATP system without knowledge of its exact phase diagram. After discovering the dependence of polymer molecular weight on the partition of SWCNTs, we are able to identify a new PEG1.5kDa/DX250kDa ATP system that is compatible for the DNA-SWCNT sorting. The high stability of the DNA-SWCNT dispersion in this ATP system allows us to realize multistage sorting of DNA-SWCNTs with minimum interfacial trapping and to look deeper into the sorting mechanism, both of which were not feasible with the previous PEG/PAM system.

## MATERIALS AND METHODS

ssDNA was purchased from Integrated DNA Technologies. CoMoCAT SWCNT powders (SG65i grade, lot no. SG65i-L46, and EG150X grade, lot no. L4) were obtained from Southwest

Nanotechnologies. Sodium chloride (NaCl; BDH Chemicals), polyethylene glycol (PEG, MW 6 kDa, Alfa Aesar), polyethylene glycol (PEG, MW 2 kDa, Alfa Aesar), polyethylene glycol (PEG, MW 1.5 kDa, Alfa Aesar), dextran 40k (DX, MW 40 kDa, TCI), dextran 70k (DX, MW 70 kDa, TCI), dextran 250k (DX, MW 250 kDa, Alfa Aesar), dextran 500k (DX, MW 500 kDa, Alfa Aesar), polyvinylpyrrolidone (PVP, MW 10 kDa, Sigma-Aldrich), polyvinylpyrrolidone (PVP, MW 40 kDa, Sigma-Aldrich), sodium phosphate ( $\text{Na}_3\text{PO}_4$ , Sigma-Aldrich), sodium phosphate dibasic ( $\text{Na}_2\text{HPO}_4$ , Sigma-Aldrich), sodium phosphate monobasic ( $\text{NaH}_2\text{PO}_4$ , Sigma-Aldrich), phosphoric acid ( $\text{H}_3\text{PO}_4$ , 85%, MCB Reagents), hydrochloric acid (HCl, Fisher Scientific), and sodium hydroxide (NaOH, Mallinckrodt Chemicals) were used as received.

DNA-SWCNT dispersions were prepared according to the previously published procedures.<sup>44,73</sup> CoMoCAT SWCNT powders were dispersed in aqueous DNA and salt solutions by sonication. Typically, the SWCNT concentration was 1 mg/mL, the SWCNT/DNA mass ratios were 1:2.5 for SG65i and 1:2 for EG150X, and the salt (NaCl) concentration was 30 mM.

For each ATP system, we need to first identify an operating condition proximal to the critical point in the phase diagram for SWCNT separation. Before sorting procedures, two ATP stock solutions denoted by 10:0 and 7:3 should be prepared. The polymer composition of 10:0 solution corresponds to the operating condition for SWCNT separation, and the composition of the 7:3 solution is calculated according to the condition that 7 parts in weight of the 7:3 solution plus 3 parts in weight of water or SWCNT dispersion yields the same polymer composition as the 10:0 solution. The compositions of the 10:0 and 7:3 stock solutions we used in this work are listed in Table 1. In a typical separation, 3 volumes (typically

**Table 1.** ATP 10:0 and 7:3 Stock Solutions Used in This Work<sup>a</sup>

ATP system	polymer, MW	10:0 mass %	7:3 mass %
PEG1.5kDa/DX250kDa	PEG, 1.5 kDa	8.57	12.2
	DX, 250 kDa	10.1	14.4
PEG6kDa/DX40kDa	PEG, 6 kDa	10.4	14.8
	DX, 40 kDa	5.52	7.88
PEG6kDa/DX70kDa	PEG, 6 kDa	5.50	7.86
	DX, 70 kDa	7.50	10.7
PEG6kDa/DX250kDa	PEG, 6 kDa	4.03	5.76
	DX, 250 kDa	8.19	11.7
PEG6kDa/DX500kDa	PEG, 6 kDa	4.06	5.80
	DX, 500 kDa	6.40	9.14
PEG/PAM	PEG, 6 kDa	7.76	11.1
	PAM, 10 kDa	15.0	21.4

<sup>a</sup>The concentrations listed here are determined at the 20 °C temperature set in our lab. Adjustment should be made if one works at a different temperature.

60  $\mu\text{L}$ ) of SWCNT dispersion is loaded to 7 volumes (typically 140  $\mu\text{L}$ ) of the 7:3 stock solution. The difference in density between SWCNT dispersion and polymer solutions can be neglected for small volumes used in separation. After phase separation, the top and bottom phases of the 10:0 stock solution should be stored separately and used as the blank top and bottom phases in the subsequent sorting procedures. The detailed preparation process of the ATP systems is given in the Supporting Information (SI).

In a multistep separation, after loading 3 volumes of the SWCNT dispersion to 7 volumes of the 7:3 stock solution, the first top fraction is extracted out. Then, the blank top phase and the modulating agents such as polyvinylpyrrolidone (PVP) are sequentially added. After vortex mixing and gentle centrifugation, a new top phase is formed and extracted. This process can be repeated multiple times to achieve the desired separation.

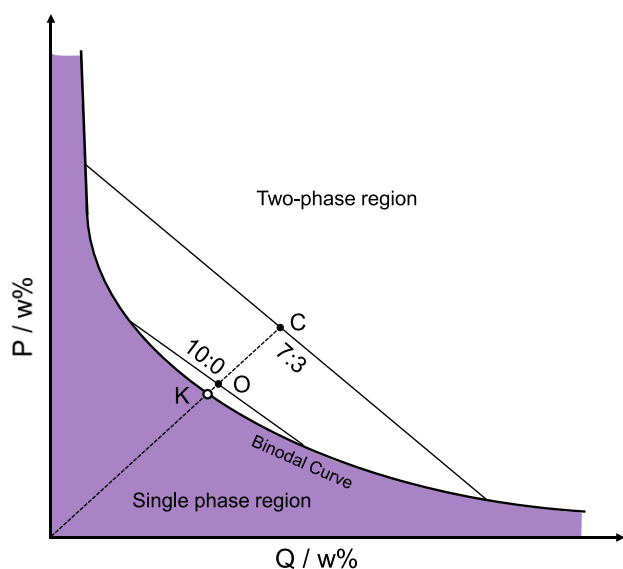
UV–vis–NIR absorption spectra were collected on a Cary 5000 spectrophotometer over the wavelength range of 200–1400 nm in 1

nm increments using a 10 mm path length quartz microcuvette. Typically, each fraction obtained during the separation was diluted by a factor of 10 before measurement. Blank top and bottom phases of the corresponding ATP system were also diluted by a factor of 10 and used as the baseline.

## RESULTS AND DISCUSSION

**Exploration and Evaluation of ATP Systems.** Scheme 1 shows the phase diagram of an ATP system made of water and

**Scheme 1. Schematic Phase Diagram of an ATP System Made of Water and Two Polymers P and Q**



two polymers P and Q. Our task is to find a good operating condition O at which the separation of SWCNTs should be operated without prior knowledge of the binodal curve. A good operating condition should be close to the critical point K of the ATP system in order to reduce the cost and the overall viscosity of the solution and to keep an  $\approx 1:1$  volume ratio of the top phase to bottom phase. However, the good operating condition should not be too close to the critical point because otherwise the composition of the ATP system may easily shift from the two-phase region to the single-phase region in the subsequent sorting procedure. Due to the lack of the corresponding phase diagram for a new ATP system and the fact that the polydispersity of the polymer might differ from batch to batch, the operating condition needs to be determined empirically. Scheme S1 depicts the general exploration procedure for a new ATP system to locate the good operating condition O near the critical point K from any starting point A, by sequentially mixing two concentrated polymer solutions, diluting, then adding the corresponding polymer, and so on. Detailed information is provided in the SI. We then separate SWCNTs at the determined good operating condition O in this new ATP system, which is denoted as the 10:0 stock solution. The composition of the more concentrated 7:3 stock solution C can be calculated by extrapolation.

We search for an “ideal” ATP system for SWCNT sorting by the following criteria: First, SWCNT dispersions should be stable in the system; otherwise, precipitation or interfacial trapping will occur and make sorting or multistage sorting impossible; second, the components of the system should be inexpensive and commercially available; and third, in order for

the large number of DNA recognition sequences identified previously in the PEG/PAM system to be compatible with the new system, the sorting result in the new system should be similar to that in the PEG/PAM system.

In this work, we use two previously identified DNA sequences to test the new ATP systems. One is A/T-based (TTA TAT TAT ATT), and the other is C/T-based (TTT CCC TTT CCC CCC). In the PEG/PAM system, left- and right-handed (6,5) and (8,3) enantiomers<sup>45</sup> were obtained with SWCNT dispersions made with these two sequences from the top and the bottom phase, respectively (Figure S1). For these reasons we call TTA TAT TAT ATT and TTT CCC TTT CCC CCC the (6,5) and (8,3) super sequences, respectively. We expect that an ideal new ATP system should also give the same separation results for these two super sequences.

**Reduced Interfacial Trapping in PEG/DX ATP Systems.** Interfacial trapping, i.e., analytes to be sorted becoming trapped at the interface preventing their equilibrium partitioning in the two phases, is a common but not well-understood phenomenon. In Albertsson’s book,<sup>48</sup> interfacial trapping of particles was attributed to inappropriate surface tensions between the particle and the two phases and between the two phases themselves. For the DNA-SWCNT dispersion, the stability of the dispersion plays an important role in affecting the interfacial trapping. The polymer type may affect the stability of the DNA-SWCNT dispersion. Compared with the PEG/PAM system, the PEG/DX system shows significantly reduced overall interfacial trapping. However, the popular PEG6kDa/DX70kDa system widely used for sorting surfactant-coated SWCNTs<sup>44</sup> failed to work for the chirality sorting of DNA-SWCNTs because the hybrids prefer heavily the bottom DX-rich phase,<sup>45</sup> and the large amount of PVP needed to extract the SWCNTs from the bottom phase to top phase often leads to poor resolution of this system. Since the molecular weight of a polymer strongly affects the partition behavior, we hypothesize that a solution could entail choosing PEG and DX of proper molecular weights.

**Effect of Polymer Molecular Weight.** The PEG/DX ATP systems consist of a PEG-rich top phase and a DX-rich bottom phase (Figure 1a). We find that the molecular weights of DX and PEG strongly affect the partition behavior of a DNA-SWCNT dispersion in the PEG/DX ATP system. Figure 1b shows the absorption spectra of the 2T fraction of four ATP combinations formed by PEG6kDa with DX40kDa, DX70kDa, DX250kDa and DX500kDa. As the molecular weight of DX increases, more (6,5) appears in the top phase. This implies that the SWCNTs are increasingly repelled by the bottom phase. Figure 1c gives the absorption spectra of the 2T fraction of three ATP combinations formed by DX250kDa with PEG1.5kDa, PEG2kDa, and PEG6kDa, respectively. The molecular weight of PEG shows a reverse effect on the partition behavior of the DNA-SWCNT dispersion. Although not as dramatic as the effect of DX molecular weight, the overall trend is that less (6,5) partitions into the top phase as the molecular weight of PEG increases. PEG with an average molecular weight less than 1.5 kDa (such as PEG1kDa, PEG600Da, and PEG400Da) will precipitate DX and thus form an aqueous/solid two-phase making the ATP extraction impossible. Using the previously identified (6,5) and (8,3) super sequences and corresponding SWCNT dispersions to test different molecular weight combinations of PEG and DX, we found PEG1.5kDa/

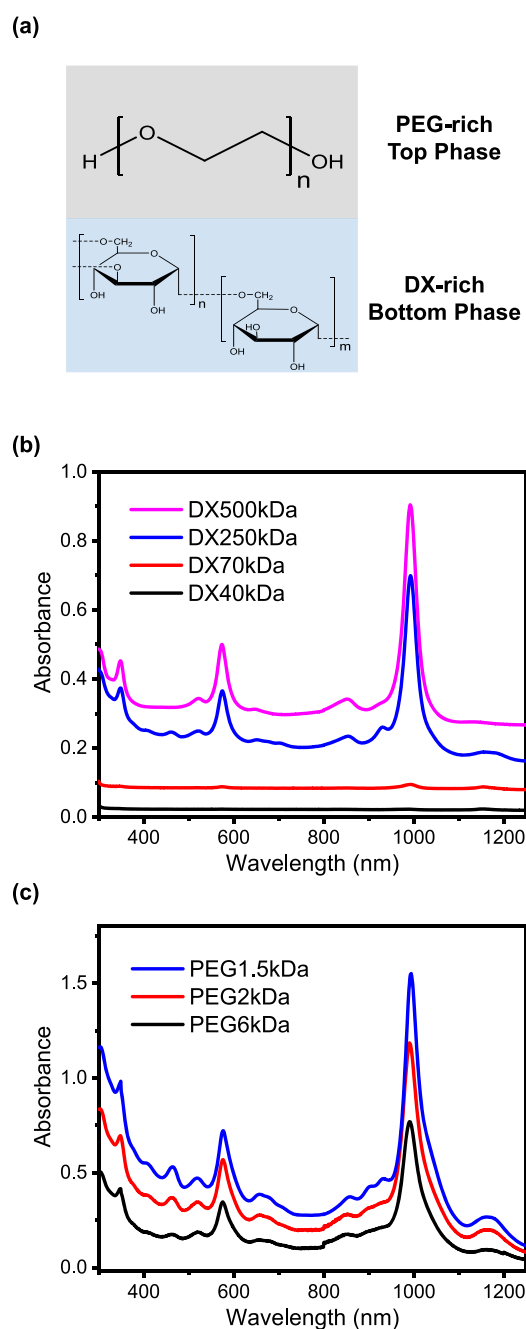


**Figure 1.** (a) Schematic illustration of PEG/DX systems, in which the top phase is PEG-rich and the bottom phase is Dextran-rich. Absorbance spectra of the first top fraction obtained after loading TTA TAT TAT ATT-SG65i (in 0.1 M NaCl) in (b) PEG6kDa/DX40kDa, PEG6kDa/DX70kDa, PEG6kDa/DX250kDa, and PEG6kDa/DX500kDa and (c) PEG1.5kDa/DX250kDa, PEG2kDa/DX250kDa, and PEG6kDa/DX250kDa at the same PVP concentration.

DX250kDa to be the best combination able to sort enantiomers of (6,5) and (8,3) from the top and bottom phases at the same time (see absorption spectra of the top and bottom phases from different PEG/DX ATP systems in Figures S2 and S3.). The mechanism of enantiomer separation is thought to be due to the different wrapping structures of the chiral DNA on left- and right-handed enantiomers.<sup>45</sup>

**PEG1.5kDa/DX250kDa ATP System.** Compared with the PEG/PAM system, the PEG1.5kDa/DX250kDa system has the following advantage: DNA-SWCNT dispersion is very

stable in the PEG1.5kDa/DX250kDa system. Among all the DNA-SWCNT dispersions tested, no visible interfacial trapping is observed in this system, while severe interfacial trapping happens in the PEG/PAM system for some dispersions (Figure S4a,b). This allows us to perform multistep sorting and obtain more kinds of pure chiralities from the bottom phases of the PEG1.5kDa/DX250kDa system. CTT CCC TTC is a sequence identified before for the purification of (9,4).<sup>45</sup> In the PEG1.5kDa/DX250kDa system, although the purity of (9,4) separated from the top phase is not as good as that from PEG/PAM system (Figure S4d), the spectra obtained from the final bottom fraction indicate that the purity of (6,6) is significantly higher in the bottom phase of PEG1.5kDa/DX250kDa than that of PEG/PAM (Figure S4e). Another example (Figure S4f) is that pure (7,5) can be obtained from the bottom phase of PEG1.5kDa/DX250kDa by using a previously identified (7,5) recognition sequence (ATT)<sub>4</sub>. Previously (ATT)<sub>4</sub>-(7,5) could only be purified from the more complex (PEG+PEG-DA)/DX ATP system.<sup>44</sup>

**Multistep Sorting of the DNA-SWCNT Dispersion.** The high stability of the DNA-SWCNT dispersion in the PEG1.5kDa/DX250kDa system enables multistage sorting without losing SWCNTs caused by interfacial trapping. Here, we use the (TCTCCC)<sub>2</sub>TCT-SG65i dispersion to demonstrate such a capability. Figure 2a shows the overall elution profile of this dispersion in the PEG1.5kDa/DX250kDa system. In a 600  $\mu\text{L}$  scale separation, at the very beginning all the SWCNTs exist in the bottom phase. By adding 0.015 mg of PVPI0kDa, we obtain the second top fraction 2T containing pure (7,3) (Figures 2b,c). Continuously adding PVP10 kDa and extracting the top phase out, we obtained fractions 3T–6T. The 6T is a (6,5)-enriched fraction, which can be further purified to obtain pure (6,5). The absorption spectra of fractions obtained from further purification of 6T are shown in Figure 2d. At the 10th step, by adding 1.5  $\mu\text{L}$  of 1 M pH = 7 sodium phosphate buffer and 0.02 mg of PVP10 kDa, a 10T fraction highly enriched in (7,4) is obtained. Then sodium phosphate buffer and PVP10 kDa are sequentially added to the solution until the bottom phase contains mainly (10,0). The detailed sorting procedure is provided in Table S1. Figure 2c is the 2D map plotted using the data in Figure 2a, from which the elution order of different carbon nanotube species can be clearly seen. Overall, in the PEG1.5kDa/DX250kDa system, four kinds of pure SWCNTs are sorted from a single (TCTCCC)<sub>2</sub>TCT-SG65i dispersion. This is the first example showing that more than two kinds of SWCNTs can be resolved from a single DNA-SWCNT dispersion. To remove the wrapping DNA, we first precipitate the DNA-SWCNT from the top phase of the PEG/DX system by adding NaSCN. After resuspension of the precipitated DNA-SWCNTs, DNA can be washed off by surfactants such as sodium deoxycholate.

**Sorting SWCNTs Wrapped by C-Rich Sequences: pH Dependence.** The preparation conditions of DNA-SWCNT dispersions are expected to affect the sorting outcome. Here, we use the PEG1.5kDa/DX250kDa system to demonstrate that DNA-SWCNT dispersions in different phosphate pH buffers greatly influence the purification of (11,0) by C-rich sequences. It is known that phosphate anions partition preferentially into the DX-rich bottom phase in the PEG/DX system, thus inducing an electrostatic potential difference between the top phase and the bottom phase.<sup>74–77</sup> The first possible effect of pH may arise from its influence on the concentrations of phosphate and mono- and dibasic phosphate

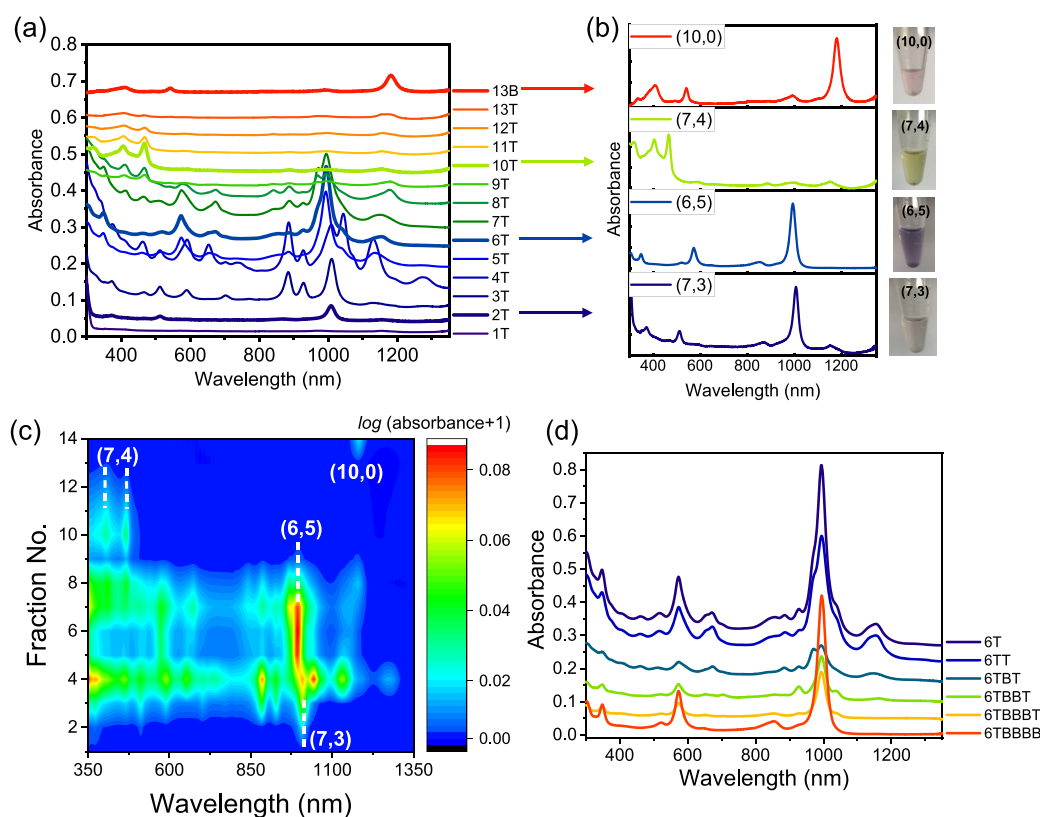


**Figure 2.** (a) Absorption spectra of each fraction obtained with continuous addition of PVP during the sorting of (TCTCCC)<sub>2</sub>TCT-SG65i (in 30 mM NaCl) in PEG1.5k/DX250k. (b) Absorption spectra and photographs of (7,3), (6,5), (7,4), and (10,0) corresponding to the 2T fraction, fraction purified from 6T, 10T fraction, and 13B fraction, respectively. (c) Contour plot of the spectra shown in part a. (d) Further purification of the 6T fraction shown in part a.

species. The second effect may come from protonation of cytidine. The  $pK_a$  of cytidine is shown in Figure 3a. For poly C sequences, their pH titration curves clearly show a two-step process (one at pH 5.7 and the other at pH 3.0).<sup>78</sup> Under low pH conditions, cytidine will be partially protonated and a hemiprotonated C-C<sup>+</sup> base pair may form intermolecular hydrogen bonding (Figure 3b,c). Formation of such hydrogen bonding has been shown by X-ray diffraction,<sup>79–81</sup> NMR,<sup>82,83</sup> and IR measurements<sup>78,84–91</sup> and is consistent with our own Fourier transform infrared spectroscopy (FTIR) of GC<sub>11</sub>-SWCNT and C<sub>12</sub>-SWCNT dispersions made in pH = 7 and pH = 4 sodium phosphate solutions (Figure S6). As a result, the pH condition is expected to have a strong influence on the sorting result. A few C-rich sequences (GC<sub>11</sub>, AC<sub>11</sub>, C<sub>12</sub>, etc.) have been identified previously in the PEG/PAM system which show the selection of (11,0). However, the GC<sub>11</sub>-SWCNT dispersion usually suffers from low yield in NaCl solution.<sup>45</sup> By using sodium phosphate buffer instead of NaCl, the yield of the C-rich sequences-SWCNT dispersion is greatly improved. Figure S5a,b shows the absorption and normalized absorption spectrum of GC<sub>11</sub>-EG150x dispersions made by using 0.1 M NaCl and 30 mM sodium phosphate buffer of different pH values. Figure 3d shows the absorption spectra of the first top fractions sorted from GC<sub>11</sub>-EG150x dispersions made in 30 mM phosphate buffer of different pH values in the PEG1.5kDa/DX250kDa ATP system (these dispersions were found to immediately aggregate once loaded into the PEG/PAM system). We find that, in the PEG1.5kDa/DX250kDa ATP system, GC11 and some other C-rich sequences (AC<sub>11</sub>,

C<sub>12</sub>, etc.) always show a good selection of (11,0) in pH = 4 phosphate buffer (Figures 3d and S5f).

One possible explanation for a better sorting outcome is that, at a low pH condition, the protonation of C bases may allow the formation of intra- or interstrand hydrogen bonding resulting in tighter and more ordered wrapping structures (Figure 3c) on SWCNTs, leading to better resolution in the PEG1.5kDa/DX250kDa system. This hypothesis of better wrapping is also consistent with the better resolution of their absorption spectra under low pH conditions (Figures S5a,b). Although the better resolution under lower pH is not so obvious for other C-rich sequences (Figure S5d–k), this trend is still roughly maintained. Previous MD simulations<sup>66–68</sup> also demonstrate that hydrogen bonding enables DNA to form a tighter and self-stitch wrapping structure on the specific SWCNT. In Figure S5b, we show that the resolution of the absorption spectrum gradually improves as the pH of the phosphate buffer varies from 8 to 6. As the pH lowers to less than 6, the resolution was maintained roughly at the same level. This indicates that dispersing SWCNTs in low pH sodium phosphate buffer by a C-rich sequence yields a better dispersion. The better wrapping under low pH in turn reduces the spread of the hydration energy of GC<sub>11</sub>-SWCNTs which improves overall separation resolution. The special behavior of the C-rich sequence is also observed by Salem et al.,<sup>92</sup> who reported sequence-dependent structural changes induced by changes in the solution ionic strength. Among all the sequences tested, the C-rich sequence shows an abnormal response to the salt concentration and pH: reducing salt concentration or lowering the pH results in an increase in the

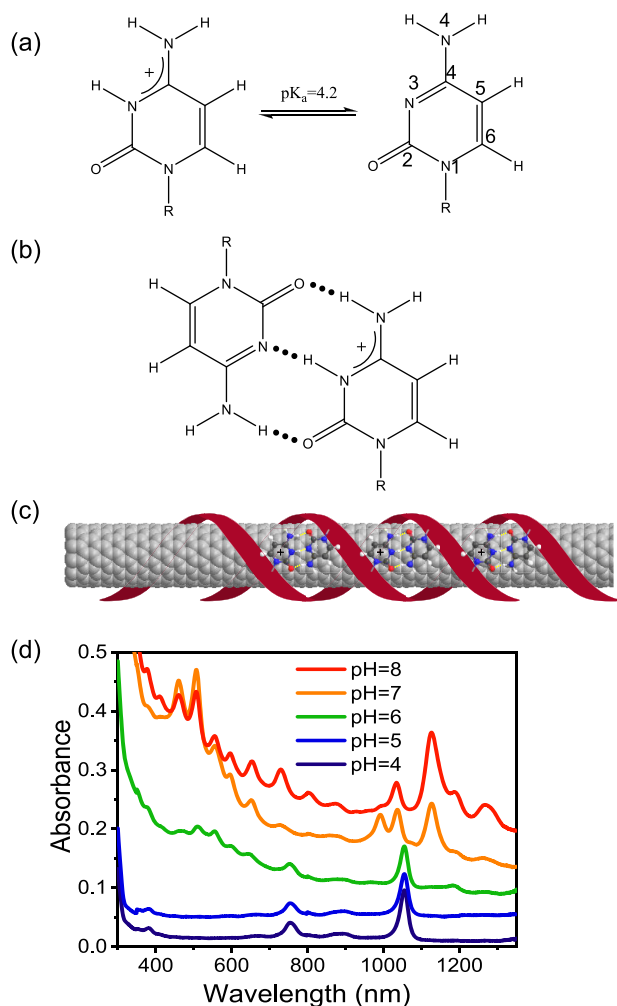


**Figure 3.** (a)  $pK_a$  values of cytosine. (b) Possible hydrogen bonding formed between hemiprotonated C–C<sup>+</sup> base pairs. (c) Schematic of C-rich sequence wrapped around (11,0)'s surface in the presence of interstrand hydrogen bonding. (d) Absorption spectra of the first top fractions obtained from GC<sub>11</sub>-SWCNTs in different pH 30 mM sodium phosphate buffers in the PEG1.5kDa/DX250kDa ATP system.

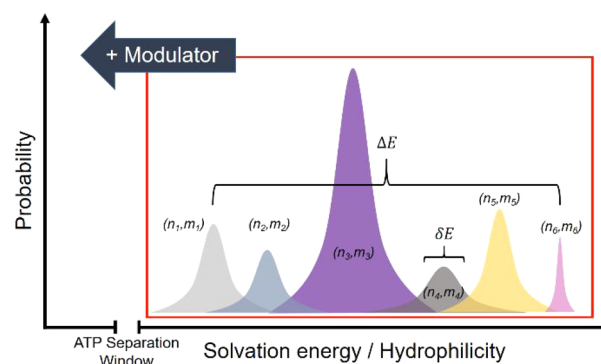
photoluminescence of the SWCNTs. They attribute this phenomenon to the protonation of the cytosine group. Further experiments showed that the amount of DNA kicked off from the nanotube surface while lowering the salt concentration is greatly reduced for C-rich sequences. Their results corroborate with our observations based on absorption spectroscopy and ATP separation. In general, the pH effect on sorting appears to be complex, highly dependent on DNA sequences and the targeting SWCNT chiralities. We found that other C-containing sequences previously identified in the PEG/PAM system for the selection of other chiralities (such as TTT CCC TTT CCC CCC for (8,3) and CTT CCC TTC for (9,4))<sup>44</sup> do not show the same trend as the C-rich sequences (Figure S5i,j).

**Recognition vs Resolving Sequences.** The notion of SWCNT recognition by specific DNA sequences was first proposed in 2009,<sup>5</sup> in order to convey the idea that a certain DNA sequence is able to form an ordered structure on one particular SWCNT chirality. This concept was able to explain most IEX data and is also consistent with many observations.

The ATP-based separation, however, gives rise to many results that cannot be simply explained by this concept. Sometimes, in the previously developed PEG/PAM system, a sequence allows two species to be purified through multistage extraction. One example is the purification of (8,4) and (7,4) from (GT)<sub>20</sub>-SWCNTs,<sup>44</sup> and another is the purification of left-handed and right-handed (6,5) from TTA TAT TAT ATT-SWCNTs.<sup>45</sup> Our new result of purification of four SWCNT species in the PEG1.5kDa/DX250kDa system from a single dispersion makes it even more clear that the concept of recognition sequences is too narrow for understanding the sorting mechanism.

We propose that it is more accurate to describe the role of specific DNA sequences as “resolving” instead of “recognizing” SWCNTs. To make this point clear, we consider the solvation energy spectrum<sup>93</sup> shown in Scheme 2. It represents the

### Scheme 2. Solvation Energy Distribution of Individual DNA-SWCNT Species, the Separation Window, and the Effect of Modulator



distribution of solvation energy of a given DNA-SWCNT dispersion. For a given DNA sequence, each DNA-(n,m) hybrid may have a distribution of solvation energy around a mean value instead of a single fixed value, because the wrapping structure of DNA on the SWCNT may adopt many conformations. The mean solvation energy values of different (n,m) species in a synthetic mixture wrapped by the same DNA are expected to have a certain spread, forming a spectrum as shown in Scheme 2. An ordered coating structure on a species (n,m) is expected to yield a narrower solvation energy distribution and, thus, is less likely to overlap with other species, making it easier to be purified from a mixture. Furthermore, if the DNA-(n,m) species happens to be at one of the two extreme ends of the spectrum (such as the species labeled (n<sub>6</sub>, m<sub>6</sub>) in Scheme 2), it will stand a better chance to be isolated. This situation corresponds to many sorting phenomena we observe in PEG/PAM system. In general, as long as a DNA sequence forms an ordered assembly on the surface of a certain SWCNT rendering a lower probability to overlap with the others in the solvation energy spectrum, this DNA-SWCNT species is more likely to be separable, no matter where its mean solvation energy is located in the solvation energy spectrum, provided that interfacial trapping is minimized to allow multistage extraction.

Interfacial trapping in PEG/PAM prevents us from assessing the resolving power for many sequences. Irreversible adsorption in IEX also causes the same problem. This problem has restricted us to purify only those ordered hybrid structures that have extreme solvation energies, which in turn gives rise to the misleading notion that one sequence can only allow one

particular (n,m) species to be purified. The PEG1.5kDa/DX250kDa system solves this problem. Sequences with high resolving power can be identified by the SWCNT sorting experiments using this newly developed PEG1.5kDa/DX250kDa system. Quantitatively, we may define the resolving power of a given DNA sequence as  $R = \Delta E / \langle \delta E \rangle$ , where  $\Delta E$  is the overall range in solvation energy and  $\langle \delta E \rangle$  is the average of  $\delta E$ , which is the solvation energy full width at half-maximum (fwhm) of the individual hybrids (Scheme 2). The quantity  $R$  may allow us to compare the resolving power of different sequences in the future.

In Scheme 2, we also draw an ATP separation window, which is defined by the intrinsic parameters of an ATP system, in order to provide a simple phenomenological description of the sorting process. If all the solvation energy peaks locate at the right side (more hydrophilic side) of this window, all species will stay in the more hydrophilic bottom phase. In contrast, if all of the peaks locate at the left side (more hydrophobic side) of this window, all SWCNTs will stay in the less hydrophilic top phase. If a peak spreads across the ATP separation window, the corresponding species will partition between the top and the bottom phases. For the PEG1.5kDa/DX250kDa system, in most cases, the initial distribution exists on the right side of its separation window, which means that all the SWCNTs stay in the bottom phase after they are loaded onto the ATP system. By adding modulators such as PVP, the initial distribution is dragged to the left (more hydrophobic side) as a whole. Ideally, since the amount of PVP added is little, its impact on the relative position of different species is negligible. With gradual increase of the PVP content, SWCNTs are sequentially brought to the top phase until the last pure fraction or nothing is left in the bottom phase. At this point, a typical sorting experiment is finished.

## CONCLUSION AND OUTLOOK

This work provides a simple yet effective method to explore ATP systems by locating a good operating condition without knowledge of the corresponding phase diagram. Based on this method, we have prepared several PEG/DX ATP systems. The molecular weights of the polymers in these ATP systems have been proven to affect the sorting results of DNA-SWCNTs. A new ATP system of PEG1.5kDa/DX250kDa has been shown to work for the chirality sorting of DNA-SWCNTs. In this system, we realize the first example of continuous multistep sorting of four SWCNT species: (7,3), (6,5), (7,4), and (10,0). In addition, the pH dependent sorting outcome suggests that the hydrogen bonding formed between hemiprotonated C–C<sup>+</sup> base pairs in some C-rich sequences may result in a tighter and more ordered wrapping structure to enable better purification SWCNTs under low pH conditions.

However, some DNA-SWCNTs do show different sorting results in this new PEG1.5kDa/DX250kDa system compared with PEG/PAM system. This means that some of the previously identified DNA sequences might not be suitable for the separation of their corresponding SWCNTs in PEG1.5kDa/DX250kDa. A systematic screen of the DNA library is needed in this new PEG/DX system, which may lead to the discovery of sequences with even higher resolving power. This will not only push DNA-based SWCNT sorting toward complete resolution of the synthetic mixture but also provide the sequences needed for the construction of a molecular perceptron to enable multiplex sensing by DNA-SWCNT dispersions.<sup>94</sup>

## ASSOCIATED CONTENT

### Supporting Information

The Supporting Information is available free of charge at <https://pubs.acs.org/doi/10.1021/jacs.9b09953>.

Details about the exploration of the ATP system, the preparation of ATP systems, absorption spectra, and FTIR spectra (PDF)

## AUTHOR INFORMATION

### Corresponding Authors

\*[yang\\_juan@pku.edu.cn](mailto:yang_juan@pku.edu.cn)

\*[yanli@pku.edu.cn](mailto:yanli@pku.edu.cn)

\*[ming.zheng@nist.gov](mailto:ming.zheng@nist.gov)

### ORCID

Juan Yang: 0000-0001-5502-9351

Yan Li: 0000-0002-3828-8340

Ming Zheng: 0000-0002-8058-1348

### Notes

The authors declare no competing financial interest.

## ACKNOWLEDGMENTS

This research is supported in part by the National Natural Science Foundation of China (Grants 21873008 and 21631002). M.L. thanks the China Scholarship Council for providing a scholarship to pursue his study at the US National Institute of Standards and Technology as a joint Ph.D. student. We also thank Dr. Gang Liu for identifying the (8,3) super sequence used in this work and Drs. Jeffrey Fagan and Prakrit Jena for their critical reading of the manuscript.

## REFERENCES

- (1) Saito, R.; Dresselhaus, G. S.; Dresselhaus, M. S. *Physical properties of carbon nanotubes*; Imperial College Press: London, 1998.
- (2) Zheng, M.; Jagota, A.; Strano, M. S.; Santos, A. P.; Barone, P.; Chou, S. G.; Diner, B. A.; Dresselhaus, M. S.; McLean, R. S.; Onoa, G. B.; Samsonidze, G. G.; Semke, E. D.; Usrey, M.; Walls, D. J. Structure-based carbon nanotube sorting by sequence-dependent DNA assembly. *Science* **2003**, *302*, 1545–1548.
- (3) Zheng, M.; Jagota, A.; Semke, E. D.; Diner, B. A.; McLean, R. S.; Lustig, S. R.; Richardson, R. E.; Tassi, N. G. DNA-assisted dispersion and separation of carbon nanotubes. *Nat. Mater.* **2003**, *2*, 338–342.
- (4) Tu, X.; Hight Walker, A. R.; Khripin, C. Y.; Zheng, M. Evolution of DNA Sequences Toward Recognition of Metallic Armchair Carbon Nanotubes. *J. Am. Chem. Soc.* **2011**, *133*, 12998–13001.
- (5) Tu, X. M.; Manohar, S.; Jagota, A.; Zheng, M. DNA sequence motifs for structure-specific recognition and separation of carbon nanotubes. *Nature* **2009**, *460*, 250–253.
- (6) Tu, X. M.; Zheng, M. A DNA-Based Approach to the Carbon Nanotube Sorting Problem. *Nano Res.* **2008**, *1*, 185–194.
- (7) Zheng, M.; Semke, E. D. Enrichment of single chirality carbon nanotubes. *J. Am. Chem. Soc.* **2007**, *129*, 6084–6085.
- (8) Penzo, E.; Palma, M.; Chenet, D. A.; Ao, G. Y.; Zheng, M.; Hone, J. C.; Wind, S. J. Directed Assembly of Single Wall Carbon Nanotube Field Effect Transistors. *ACS Nano* **2016**, *10*, 2975–2981.
- (9) Penzo, E.; Palma, M.; Wang, R. S.; Cai, H. G.; Zheng, M.; Wind, S. J. Directed Assembly of End-Functionalized Single Wall Carbon Nanotube Segments. *Nano Lett.* **2015**, *15*, 6547–6552.
- (10) Han, S.-p.; Maune, H. T.; Barish, R. D.; Bockrath, M.; Goddard, W. A., III DNA-linker-induced surface assembly of ultra dense parallel single walled carbon nanotube arrays. *Nano Lett.* **2012**, *12*, 1129–1135.
- (11) Maune, H. T.; Han, S.-p.; Barish, R. D.; Bockrath, M.; Goddard, W. A., III; Rothmund, P. W.; Winfree, E. Self-assembly of

carbon nanotubes into two-dimensional geometries using DNA origami templates. *Nat. Nanotechnol.* **2010**, *5*, 61–66.

(12) Pei, H.; Sha, R.; Wang, X.; Zheng, M.; Fan, C.; Canary, J. W.; Seeman, N. C. Organizing End-Site-Specific SWCNTs in Specific Loci Using DNA. *J. Am. Chem. Soc.* **2019**, *141*, 11923–11928.

(13) Staii, C.; Johnson, A. T.; Chen, M.; Gelperin, A. DNA-decorated carbon nanotubes for chemical sensing. *Nano Lett.* **2005**, *5*, 1774–1778.

(14) Jeng, E. S.; Moll, A. E.; Roy, A. C.; Gastala, J. B.; Strano, M. S. Detection of DNA hybridization using the near-infrared band-gap fluorescence of single-walled carbon nanotubes. *Nano Lett.* **2006**, *6*, 371–375.

(15) Heller, D. A.; Jeng, E. S.; Yeung, T.-K.; Martinez, B. M.; Moll, A. E.; Gastala, J. B.; Strano, M. S. Optical detection of DNA conformational polymorphism on single-walled carbon nanotubes. *Science* **2006**, *311*, 508–511.

(16) Zhang, J.; Boghossian, A. A.; Barone, P. W.; Rwei, A.; Kim, J.-H.; Lin, D.; Heller, D. A.; Hilmer, A. J.; Nair, N.; Reuel, N. F.; Strano, M. S. Single molecule detection of nitric oxide enabled by d(AT) 15 DNA adsorbed to near infrared fluorescent single-walled carbon nanotubes. *J. Am. Chem. Soc.* **2011**, *133*, 567–581.

(17) Heller, D. A.; Jin, H.; Martinez, B. M.; Patel, D.; Miller, B. M.; Yeung, T.-K.; Jena, P. V.; Höbartner, C.; Ha, T.; Silverman, S. K.; Strano, M. S. Multimodal optical sensing and analyte specificity using single-walled carbon nanotubes. *Nat. Nanotechnol.* **2009**, *4*, 114–120.

(18) Jena, P. V.; Roxbury, D.; Galassi, T. V.; Akkari, L.; Horoszko, C. P.; Iaea, D. B.; Budhathoki-Uprety, J.; Pipalia, N.; Haka, A. S.; Harvey, J. D.; Mittal, J.; Maxfield, F. R.; Joyce, J. A.; Heller, D. A. A carbon nanotube optical reporter maps endolysosomal lipid flux. *ACS Nano* **2017**, *11*, 10689–10703.

(19) Xu, X.; Clement, P.; Eklöf-Österberg, J.; Kelley-Loughnane, N.; Moth-Poulsen, K.; Chávez, J. L.; Palma, M. Reconfigurable Carbon Nanotube Multiplexed Sensing Devices. *Nano Lett.* **2018**, *18*, 4130–4135.

(20) Williams, R. M.; Lee, C.; Galassi, T. V.; Harvey, J. D.; Leicher, R.; Sirenko, M.; Dorso, M. A.; Shah, J.; Olvera, N.; Dao, F.; Levine, D. A.; Heller, D. A. Noninvasive ovarian cancer biomarker detection via an optical nanosensor implant. *Science advances* **2018**, *4*, No. eaq1090.

(21) Zhang, J.; Landry, M. P.; Barone, P. W.; Kim, J.-H.; Lin, S.; Ulissi, Z. W.; Lin, D.; Mu, B.; Boghossian, A. A.; Hilmer, A. J.; Rwei, A.; Hinckley, A. C.; Kruss, S.; Shandell, M. A.; Nair, N.; Blake, S.; Sen, F.; Sen, S.; Croy, R. G.; Li, D.; Yum, K.; Ahn, J.-H.; Jin, H.; Heller, D. A.; Essigmann, J. M.; Blankschtein, D.; Strano, M. S. Molecular recognition using corona phase complexes made of synthetic polymers adsorbed on carbon nanotubes. *Nat. Nanotechnol.* **2013**, *8*, 959–968.

(22) Arnold, M. S.; Stupp, S. I.; Hersam, M. C. Enrichment of single-walled carbon nanotubes by diameter in density gradients. *Nano Lett.* **2005**, *5*, 713–718.

(23) Arnold, M. S.; Green, A. A.; Hulvat, J. F.; Stupp, S. I.; Hersam, M. C. Sorting carbon nanotubes by electronic structure using density differentiation. *Nat. Nanotechnol.* **2006**, *1*, 60–65.

(24) Niyogi, S.; Densmore, C. G.; Doorn, S. K. Electrolyte tuning of surfactant interfacial behavior for enhanced density-based separations of single-walled carbon nanotubes. *J. Am. Chem. Soc.* **2009**, *131*, 1144–1153.

(25) Fagan, J. A.; Becker, M. L.; Chun, J.; Hobbie, E. K. Length fractionation of carbon nanotubes using centrifugation. *Adv. Mater.* **2008**, *20*, 1609–1613.

(26) Háróz, E. H.; Rice, W. D.; Lu, B. Y.; Ghosh, S.; Hauge, R. H.; Weisman, R. B.; Doorn, S. K.; Kono, J. Enrichment of armchair carbon nanotubes via density gradient ultracentrifugation: Raman spectroscopy evidence. *ACS Nano* **2010**, *4*, 1955–1962.

(27) Ghosh, S.; Bachilo, S. M.; Weisman, R. B. Advanced sorting of single-walled carbon nanotubes by nonlinear density-gradient ultracentrifugation. *Nat. Nanotechnol.* **2010**, *5*, 443–450.

(28) Fagan, J. A.; Zheng, M.; Rastogi, V.; Simpson, J. R.; Khripin, C. Y.; Silvera Batista, C. A.; Hight Walker, A. R. Analyzing surfactant structures on length and chirality resolved (6, 5) single-wall carbon

nanotubes by analytical ultracentrifugation. *ACS Nano* **2013**, *7*, 3373–3387.

(29) Lam, S.; Zheng, M.; Fagan, J. A. Characterizing the effect of salt and surfactant concentration on the counterion atmosphere around surfactant stabilized SWCNTs using analytical ultracentrifugation. *Langmuir* **2016**, *32*, 3926–3936.

(30) Chen, F.; Wang, B.; Chen, Y.; Li, L.-J. Toward the extraction of single species of single-walled carbon nanotubes using fluorene-based polymers. *Nano Lett.* **2007**, *7*, 3013–3017.

(31) Nish, A.; Hwang, J.-Y.; Doig, J.; Nicholas, R. J. Highly selective dispersion of single-walled carbon nanotubes using aromatic polymers. *Nat. Nanotechnol.* **2007**, *2*, 640–646.

(32) Ju, S.-Y.; Doll, J.; Sharma, I.; Papadimitrakopoulos, F. Selection of carbon nanotubes with specific chiralities using helical assemblies of flavin mononucleotide. *Nat. Nanotechnol.* **2008**, *3*, 356–362.

(33) Ozawa, H.; Fujigaya, T.; Niidome, Y.; Hotta, N.; Fujiki, M.; Nakashima, N. Rational concept to recognize/extract single-walled carbon nanotubes with a specific chirality. *J. Am. Chem. Soc.* **2011**, *133*, 2651–2657.

(34) Tanaka, T.; Jin, H.; Miyata, Y.; Fujii, S.; Suga, H.; Naitoh, Y.; Minari, T.; Miyadera, T.; Tsukagoshi, K.; Kataura, H. Simple and scalable gel-based separation of metallic and semiconducting carbon nanotubes. *Nano Lett.* **2009**, *9*, 1497–1500.

(35) Moshhammer, K.; Hennrich, F.; Kappes, M. M. Selective suspension in aqueous sodium dodecyl sulfate according to electronic structure type allows simple separation of metallic from semiconducting single-walled carbon nanotubes. *Nano Res.* **2009**, *2*, 599–606.

(36) Liu, H.; Nishide, D.; Tanaka, T.; Kataura, H. Large-scale single-chirality separation of single-wall carbon nanotubes by simple gel chromatography. *Nat. Commun.* **2011**, *2*, 309.

(37) Liu, H.; Tanaka, T.; Kataura, H. Optical isomer separation of single-chirality carbon nanotubes using gel column chromatography. *Nano Lett.* **2014**, *14*, 6237–6243.

(38) Khripin, C. Y.; Fagan, J. A.; Zheng, M. Spontaneous Partition of Carbon Nanotubes in Polymer-Modified Aqueous Phases. *J. Am. Chem. Soc.* **2013**, *135*, 6822–6825.

(39) Fagan, J. A.; Khripin, C. Y.; Silvera Batista, C. A.; Simpson, J. R.; Haroz, E. H.; Hight Walker, A. R.; Zheng, M. Isolation of Specific Small-Diameter Single-Wall Carbon Nanotube Species via Aqueous Two-Phase Extraction. *Adv. Mater.* **2014**, *26*, 2800–2804.

(40) Fagan, J. A.; Haroz, E. H.; Ihly, R.; Gui, H.; Blackburn, J. L.; Simpson, J. R.; Lam, S.; Hight Walker, A. R.; Doorn, S. K.; Zheng, M. Isolation of > 1 nm Diameter Single-Wall Carbon Nanotube Species Using Aqueous Two-Phase Extraction. *ACS Nano* **2015**, *9*, 5377–5390.

(41) Gui, H.; Streit, J. K.; Fagan, J. A.; Hight Walker, A. R.; Zhou, C.; Zheng, M. Redox Sorting of Carbon Nanotubes. *Nano Lett.* **2015**, *15*, 1642–1646.

(42) Subbaiyan, N. K.; Cambré, S.; Parra-Vasquez, A. N. G.; Háróz, E. H.; Doorn, S. K.; Duque, J. G. Role of surfactants and salt in aqueous two-phase separation of carbon nanotubes toward simple chirality isolation. *ACS Nano* **2014**, *8*, 1619–1628.

(43) Li, H.; Gordeev, G.; Garrity, O.; Reich, S.; Flavel, B. S. Separation of Small Diameter Single Walled Carbon Nanotubes in 1–3 Steps with Aqueous Two-Phase Extraction. *ACS Nano* **2019**, *13*, 2567–2578.

(44) Ao, G. Y.; Khripin, C. Y.; Zheng, M. DNA-Controlled Partition of Carbon Nanotubes in Polymer Aqueous Two-Phase Systems. *J. Am. Chem. Soc.* **2014**, *136*, 10383–10392.

(45) Ao, G.; Streit, J. K.; Fagan, J. A.; Zheng, M. Differentiating Left- and Right-handed Carbon Nanotubes by DNA. *J. Am. Chem. Soc.* **2016**, *138*, 16677–16685.

(46) Yang, Y.; Zheng, M.; Jagota, A. Learning to predict single-wall carbon nanotube-recognition DNA sequences. *npj Computational Materials* **2019**, *5*, 3.

(47) Fagan, J. A. Aqueous two-polymer phase extraction of single-wall carbon nanotubes using surfactants. *Nanoscale Adv.* **2019**, *1*, 3307–3324.

- (48) Albertsson, P.-Å. *Partition of cell particles and macromolecules*, 2nd ed.; Wiley-Interscience: New York, 1971.
- (49) Eiteman, M. A. Hydrophobic and charge effects in the partitioning of solutes in aqueous two-phase systems. In *Aqueous Biphasic Separations: Biomolecules to Metal Ions*; Rogers, R. D., Eiteman, M. A., Eds.; Plenum Press: New York, 1995; pp 31–48.
- (50) Albertsson, P.-Å. *Aqueous Biphasic Systems. Properties and Applications in Bioseparation*. In *Aqueous Biphasic Separations: Biomolecules to Metal Ions*; Rogers, R. D., Eiteman, M. A., Eds.; Plenum Press: New York, 1995; pp 21–30.
- (51) Huddleston, J.; Veide, A.; Köhler, K.; Flanagan, J.; Enfors, S.-O.; Lyddiatt, A. The molecular basis of partitioning in aqueous two-phase systems. *Trends Biotechnol.* **1991**, *9*, 381–388.
- (52) Asenjo, J. A.; Andrews, B. A. Aqueous two-phase systems for protein separation: a perspective. *J. Chromatogr. A* **2011**, *1218*, 8826–8835.
- (53) Matos, T.; Johansson, H.-O.; Queiroz, J. A.; Bulow, L. Isolation of PCR DNA fragments using aqueous two-phase systems. *Sep. Purif. Technol.* **2014**, *122*, 144–148.
- (54) Ventura, S. P. M.; de Barros, R. L. F.; de Pinho Barbosa, J. M.; Soares, C. M. F.; Lima, A. S.; Coutinho, J. A. P. Production and purification of an extracellular lipolytic enzyme using ionic liquid-based aqueous two-phase systems. *Green Chem.* **2012**, *14*, 734–740.
- (55) Rosa, P.; Azevedo, A.; Ferreira, I.; De Vries, J.; Korporaal, R.; Verhoef, H.; Visser, T.; Aires-Barros, M. Affinity partitioning of human antibodies in aqueous two-phase systems. *J. Chromatogr. A* **2007**, *1162*, 103–113.
- (56) Liu, C.-l.; Kamei, D. T.; King, J. A.; Wang, D. I.; Blankschtein, D. Separation of proteins and viruses using two-phase aqueous micellar systems. *J. Chromatogr., Biomed. Appl.* **1998**, *711*, 127–138.
- (57) SooHoo, J. R.; Walker, G. M. Microfluidic aqueous two phase system for leukocyte concentration from whole blood. *Biomed. Microdevices* **2009**, *11*, 323–329.
- (58) Rogers, R. D.; Eiteman, M. A. *Aqueous Biphasic Separations: Biomolecules to Metal Ions*; Plenum Press: New York, 1995.
- (59) Akbulut, O.; Mace, C. R.; Martinez, R. V.; Kumar, A. A.; Nie, Z.; Patton, M. R.; Whitesides, G. M. Separation of nanoparticles in aqueous multiphase systems through centrifugation. *Nano Lett.* **2012**, *12*, 4060–4064.
- (60) Grilo, A. L.; Raquel Aires-Barros, M.; Azevedo, A. M. Partitioning in aqueous two-phase systems: fundamentals, applications and trends. *Sep. Purif. Rev.* **2016**, *45*, 68–80.
- (61) Yang, Y.; Shankar, A.; Aryaksama, T.; Zheng, M.; Jagota, A. Quantification of DNA/SWCNT Solvation Differences by Aqueous Two-Phase Separation. *Langmuir* **2018**, *34*, 1834–1843.
- (62) Roxbury, D.; Tu, X. M.; Zheng, M.; Jagota, A. Recognition Ability of DNA for Carbon Nanotubes Correlates with Their Binding Affinity. *Langmuir* **2011**, *27*, 8282–8293.
- (63) Zheng, Y.; Bachilo, S. M.; Weisman, R. B. Enantiomers of Single-Wall Carbon Nanotubes Show Distinct Coating Displacement Kinetics. *J. Phys. Chem. Lett.* **2018**, *9*, 3793–3797.
- (64) Zheng, Y.; Bachilo, S. M.; Weisman, R. B. Quenching of Single-Walled Carbon Nanotube Fluorescence by Dissolved Oxygen Reveals Selective Single-Stranded DNA Affinities. *J. Phys. Chem. Lett.* **2017**, *8*, 1952–1955.
- (65) Johnson, R. R.; Johnson, A. C.; Klein, M. L. Probing the structure of DNA–carbon nanotube hybrids with molecular dynamics. *Nano Lett.* **2008**, *8*, 69–75.
- (66) Roxbury, D.; Mittal, J.; Jagota, A. Molecular-basis of single-walled carbon nanotube recognition by single-stranded DNA. *Nano Lett.* **2012**, *12*, 1464–1469.
- (67) Roxbury, D.; Jagota, A.; Mittal, J. Structural characteristics of oligomeric dna strands adsorbed onto single-walled carbon nanotubes. *J. Phys. Chem. B* **2013**, *117*, 132–140.
- (68) Roxbury, D.; Jagota, A.; Mittal, J. Sequence-specific self-stitching motif of short single-stranded DNA on a single-walled carbon nanotube. *J. Am. Chem. Soc.* **2011**, *133*, 13545–13550.
- (69) Zhang, M.; Khripin, C. Y.; Fagan, J. A.; McPhie, P.; Ito, Y.; Zheng, M. Single-Step Total Fractionation of Single-Wall Carbon Nanotubes by Countercurrent Chromatography. *Anal. Chem.* **2014**, *86*, 3980–3984.
- (70) Streit, J.; Snyder, C. R.; Campo, J.; Zheng, M.; Simpson, J. R.; Hight Walker, A. R.; Fagan, J. A. Alkane Encapsulation Induces Strain in Small-Diameter Single-Wall Carbon Nanotubes. *J. Phys. Chem. C* **2018**, *122*, 11577–11585.
- (71) Campo, J.; Piao, Y.; Lam, S.; Stafford, C. M.; Streit, J. K.; Simpson, J. R.; Hight Walker, A. R.; Fagan, J. A. Enhancing single-wall carbon nanotube properties through controlled endohedral filling. *Nanoscale Horiz* **2016**, *1*, 317–324.
- (72) Luo, H.-B.; Wang, P.; Wu, X.; Qu, H.; Ren, X.; Wang, Y. One-Pot, Large-Scale Synthesis of Organic Color Center-Tailored Semiconducting Carbon Nanotubes. *ACS Nano* **2019**, *13*, 8417–8424.
- (73) Ao, G.; Zheng, M. Preparation and Separation of DNA-Wrapped Carbon Nanotubes. *Curr. Protoc. Chem. Biol.* **2015**, *7*, 43–51.
- (74) Bamberger, S.; Seaman, G. V.; Brown, J. A.; Brooks, D. E. The partition of sodium phosphate and sodium chloride in aqueous dextran poly (ethylene glycol) two-phase systems. *J. Colloid Interface Sci.* **1984**, *99*, 187–193.
- (75) Reitherman, R.; Flanagan, S. D.; Barondes, S. H. Electromotive phenomena in partition of erythrocytes in aqueous polymer two phase systems. *Biochim. Biophys. Acta, Gen. Subj.* **1973**, *297*, 193–202.
- (76) Johansson, G. Partition of salts and their effects on partition of proteins in a dextran-poly(ethylene glycol)-water two-phase system. *Biochim. Biophys. Acta, Protein Struct.* **1970**, *221*, 387–390.
- (77) Albertsson, P. Å.; Baird, G. D. Counter-current distribution of cells. *Exp. Cell Res.* **1962**, *28*, 296–322.
- (78) Hartman, K. A.; Rich, A. The Tautomeric Form of Helical Polyribocytidylic Acid. *J. Am. Chem. Soc.* **1965**, *87*, 2033–2039.
- (79) Kang, C.; Berger, I.; Lockshin, C.; Ratliff, R.; Moyzis, R.; Rich, A. Stable loop in the crystal structure of the intercalated four-stranded cytosine-rich metazoan telomere. *Proc. Natl. Acad. Sci. U. S. A.* **1995**, *92*, 3874.
- (80) Berger, I.; Kang, C.; Fredian, A.; Ratliff, R.; Moyzis, R.; Rich, A. Extension of the four-stranded intercalated cytosine motif by adenine•adenine base pairing in the crystal structure of d(CCCAAT). *Nat. Struct. Mol. Biol.* **1995**, *2*, 416–425.
- (81) Langridge, R.; Rich, A. Molecular Structure of Helical Polycytidylic Acid. *Nature* **1963**, *198*, 725–728.
- (82) Lieblein, A. L.; Krämer, M.; Dreuw, A.; Fürtig, B.; Schwalbe, H. The Nature of Hydrogen Bonds in Cytidine•H•••Cytidine DNA Base Pairs. *Angew. Chem., Int. Ed.* **2012**, *51*, 4067–4070.
- (83) Gehring, K.; Leroy, J.-L.; Guéron, M. A tetrameric DNA structure with protonated cytosine-cytosine base pairs. *Nature* **1993**, *363*, 561–565.
- (84) Petrovic, A. G.; Polavarapu, P. L. Structural Transitions in Polyribocytidylic Acid Induced by Changes in pH and Temperature: Vibrational Circular Dichroism Study in Solution and Film States. *J. Phys. Chem. B* **2006**, *110*, 22826–22833.
- (85) Panin, L. E.; Kunitsyn, V. G.; Tuzikov, F. V. Changes in the Secondary Structure of Highly Polymeric DNA and CC(GCC)<sub>n</sub>-Type Oligonucleotides under the Action of Steroid Hormones and Their Complexes with Apolipoprotein A I. *J. Phys. Chem. B* **2006**, *110*, 13560–13571.
- (86) Maleev, V.; Semenov, M.; Kashpur, V.; Bolbukh, T.; Shestopalova, A.; Anishchenko, D. Structure and hydration of polycytidylic acid from the data of infrared spectroscopy, EHF dielectrometry and computer modeling. *J. Mol. Struct.* **2002**, *605*, 51–61.
- (87) Geinguenaud, F.; Liquier, J.; Brevnov, M. G.; Petruskenskene, O. V.; Alexeev, Y. I.; Gromova, E. S.; Taillandier, E. Parallel Self-Associated Structures Formed by T<sub>1</sub>C-Rich Sequences at Acidic pH. *Biochemistry* **2000**, *39*, 12650–12658.
- (88) Gavira, J. M.; Campos, M.; Diaz, G.; Hernanz, A.; Navarro, R. Vibrational analysis and spectra of cytidine 3'-monophosphate (3'-CMP). *Vib. Spectrosc.* **1997**, *15*, 1–16.

(89) Florián, J.; Baumruk, V.; Leszczyński, J. IR and Raman Spectra, Tautomeric Stabilities, and Scaled Quantum Mechanical Force Fields of Protonated Cytosine. *J. Phys. Chem.* **1996**, *100*, 5578–5589.

(90) Liquier, J.; Letellier, R.; Dagneaux, C.; Ouali, M.; Morvan, F.; Raynier, B.; Imbach, J. L.; Taillandier, E. Triple helix formation by alpha-oligodeoxynucleotides: A vibrational spectroscopy and molecular modeling study. *Biochemistry* **1993**, *32*, 10591–10598.

(91) Zundel, G.; Lubos, W. D.; Kölkenbeck, K. Proton dispersion forces. Secondary-structure stabilizing forces between the hydrogen bonds of the polynucleotides. *Biophys. J.* **1972**, *12*, 1509–1514.

(92) Salem, D. P.; Gong, X.; Liu, A. T.; Koman, V. B.; Dong, J.; Strano, M. S. Ionic Strength-Mediated Phase Transitions of Surface-Adsorbed DNA on Single-Walled Carbon Nanotubes. *J. Am. Chem. Soc.* **2017**, *139*, 16791–16802.

(93) Zheng, M. Sorting Carbon Nanotubes. *Top. Curr. Chem.* **2017**, *375*, 13.

(94) Zheng, M. Structure-Defined DNA-Carbon Nanotube Hybrids and Their Applications. *ECS Trans.* **2018**, *85*, 511–517.